NUCL SCI TECH (2018) 29:125
https://doi.org/10.1007/s41365-018-0465-2

Influence of α-Al_2O_3 and AlF_3 on pyrohydrolysis of Li_3AlF_6

Jia Peng[1,2,3] · Xiao-Bei Zheng[1,3] · Yu-Xia Liu[1,3] · Lan Zhang[1,3]

Received: 29 November 2017 / Revised: 5 February 2018 / Accepted: 22 March 2018 / Published online: 25 July 2018

Abstract In this study, Li_3AlF_6 was employed to simulate the molten salt LiF–BeF_2 to explore its pyrohydrolysis behavior and that of its components, i.e., LiF and AlF_3, respectively. The influence of the accelerators α-Al_2O_3 and AlF_3 on the pyrohydrolysis of LiF and Li_3AlF_6 was investigated. Finally, the solid pyrohydrolytic products were characterized by means of X-ray diffraction, and the corresponding reaction mechanisms were proposed. These experimental results indicated that AlF_3 was completely hydrolyzed to the corresponding oxide α-Al_2O_3 at 650 °C in 1 h, whereas the complete hydrolysis of LiF and Li_3AlF_6 required the assistance of either α-Al_2O_3 or AlF_3 under the same conditions. The influence of the accelerator α-Al_2O_3 and AlF_3 on the pyrohydrolytic behavior of Li_3AlF_6 provides references for future research studies on the pyrohydrolysis of LiF–BeF_2 and multi-component molten salts.

Keywords Pyrohydrolysis · Accelerator · Li_3AlF_6 molten salt · Reaction mechanism

1 Introduction

Molten salt reactors (MSRs), which are generation IV reactors, are the only type of liquid fuel reactor based on the thorium–uranium fuel cycle. Compared with other breeder reactors and solid fuel reactors, an MSR exhibits the properties of higher inherent safety, higher thermoelectric conversion efficiency, less nuclear waste, and nonproliferation attributes [1, 2]. A thorium-based molten salt reactor (TMSR) is designed to take full advantage of abundant thorium resources. In a TMSR, thorium–uranium fuel is dissolved in the carrier molten salt (LiF–BeF_2) in the form of fluorides [3]. The majority of nuclear fission products produced from the thorium–uranium fuel cycle is also present in the form of fluorides. Thus, long-term storage of these products may lead to the formation of harmful substances, such as F_2 and HF [4], which significantly complicates final waste treatment. As a result, it is necessary to convert fluorides into oxides for further treatment.

Pyrohydrolysis is an acceptable procedure that is routinely used for the separation and determination of fluorides and other halides [5–8]. It is a fast, reliable, and highly convenient method for the decomposition of solid samples. The pyrohydrolysis reaction is conducted by treating a sample holder in the form of a boat containing the sample in a reaction tube with superheated steam at high temperature, and then the distillate is either cooled and collected in the receiver containing the absorbing solution [9–11] or collected at temperatures near 0 °C without using an absorbing solution [12]. Previous results from this laboratory showed that a series of single fluorides, such as UF_4, ThF_4, and ZrF_4 [13], could be converted into their corresponding oxides by using a homemade

---

This work was supported by the "Strategic Priority Research Program" of the Chinese Academy of Sciences (No. XDA02030000).

✉ Yu-Xia Liu
liuyuxia@sinap.ac.cn

✉ Lan Zhang
zhanglan@sinap.ac.cn

[1] Shanghai Institute of Applied Physics, Chinese Academy of Sciences, Shanghai 201800, China

[2] University of Chinese Academy of Sciences, Beijing 100049, China

[3] CAS Innovative Academy in TMSR Energy System, Shanghai 201800, China

apparatus for pyrohydrolysis experiments. Prior work proved the feasibility of the pyrohydrolysis method for the treatment of fluorides when reprocessing spent TMSR fuel. However, alkaline, alkaline-earth, and rare-earth fluorides are difficult to hydrolyze and require higher temperatures [5, 14]. Hence, it is necessary to develop a fast pyrohydrolysis method at low temperature for the extraction of F^- from fluoride compounds. The oxides U_3O_8, WO_3, Cr_2O_3, α-Al_2O_3, and V_2O_5, and the salts $Na_2W_2O_7$ and $Li_2W_2O_7$ have all been recommended as accelerators [5, 7, 15–18].

The behavior of fluorides from spent TMSR fuel has been investigated in the past few years. Results obtained with single fluorides showed that our homemade pyrohydrolysis device could be used to transform some single fluorides into their corresponding oxides. With respect to spent TMSR fuel, which comprises hybrid molten salts containing multiple components, the feasibility of hydrolyzing single fluorides has been validated. Therefore, further study on the pyrohydrolysis behavior of mixed molten salts needs to be carried out. This requires us to first understand the pyrohydrolysis properties of the carrier salt LiF–BeF_2.

In the carrier salt LiF–BeF_2, the fluoride BeF_2 is a toxic carcinogen and intense irritant and may release highly toxic smoke upon exposure to high temperatures or acids. In addition, experiments using BeF_2 require a series of safety assessments and approval, making it impossible to carry out LiF–BeF_2-related experiments at the moment. We therefore considered replacing Be with Al, because these two elements are positioned on a diagonal line (upper left, bottom right) in the periodic table, and would be expected to have similar properties according to the diagonal rules. Apart from this, AlF_3 and BeF_2 form similar complexes with alkali metal fluorides. For example, AlF_3 and LiF can form Li_3AlF_6 [19–22], and BeF_2 can form Li_2BeF_4 with LiF [23]. Therefore, AlF_3 was used instead of BeF_2 and LiF–BeF_2 was represented by Li_3AlF_6 in the experiment. Because of the need to avoid impurities in further treatment, no additional elements were introduced. Thus, α-Al_2O_3 was chosen as a suitable accelerator in this study. All these modifications were made with the aim of providing the necessary data and obtaining useful guidance for the subsequent pyrohydrolysis experiments of LiF–BeF_2 and other multi-component hybrid molten salts.

2 Experimental

2.1 Chemicals and reagents

α-Al_2O_3, guaranteed to be 99.99% pure, was purchased from Alfa Aesar (China) Chemical Co. Ltd. LiF and AlF_3, guaranteed to be 99.9% pure, were commercially obtained from Sigma-Aldrich (Shanghai) Trading Co., Ltd. Li_3AlF_6 (200 mesh), guaranteed to be 99% pure, was purchased from Zibo Senow Chemical Co. Ltd. NaOH was commercially obtained from Sinopharm Chemical Reagent Co., Ltd. High-purity water (18.2 MΩ·cm) from a Milli-Q water purification system (Millipore, USA) was used for all solutions through the chemical process. All the pyrohydrolysis samples are powders and guaranteed to be 200–300 mesh. The sample mass in the experiments is approximately 80–130 mg.

2.2 Apparatus

The device for the pyrohydrolysis experiments is the same as that used by Dong [13]. The main parts of the device are: the gas supply system, steam generator, high-temperature furnace, gas control system, off-gas collection equipment, and water-cooling device. All the valves, the reaction tube, and gas pipeline are manufactured of Hastelloy C276 alloy. The reaction boat, which is manufactured of platinum, is up to 50 mm in length, 40 mm in width, and 10 mm in height, and was shaped from 0.5-mm-thick platinum foil. The reaction tube is approximately 660 mm in length and 60 mm in outside diameter with a wall thickness of 1.5 mm. In the reaction tube, the heating zone in which a constant temperature is maintained is approximately 200 mm long. The carrier gas is Ar, the temperature of the steam generator is 120 °C, and the upper limit of the working temperature of the furnace is 1000 °C. The HF gas produced by the reaction was absorbed with 0.1 mol/L NaOH solution. An X'Pert powder (PANalytical, 40 kV, 40 mA, Cu Ka) X-ray diffractometer was used for XRD measurements.

2.3 Experimental procedures

Accurately weighed samples and an accelerator were evenly ground and placed in a platinum reaction boat. Our previous work revealed that the thickness of the sample layer had no effect on the pyrohydrolysis yield when the sample layer was less than 1 mm thick. Hence, the thickness of the sample layer in the reaction boat was approximately 0.3–0.8 mm. The boat was placed in the central section of the reaction chamber, and the temperature of the reaction tube was adjusted to 650 °C. The air tightness of the reaction tube was checked by using a pumped vacuum system. Superheated water with a flow rate of 2.5 mL/min was used in our experiment. When the reaction was complete, the reaction furnace was cooled to room temperature. The platinum boat was removed from the reaction tube and placed in an oven for 30 min. The reaction efficiency was calculated by using a weighing method. The solid products were structurally characterized by XRD.

3 Results and discussion

3.1 Pyrohydrolysis of AlF_3

The pyrohydrolysis yield of AlF_3 was studied at different temperatures and for various reaction times, as shown in Fig. 1a, b. It is clearly shown in Fig. 1a that the pyrohydrolysis yield significantly increased with the reaction temperature during the initial stage up to 650 °C for 1 h. Therefore, the pyrohydrolysis was conducted at the temperature of 650 °C to ensure complete hydrolysis of the sample. Figure 1b shows the relationship between the pyrohydrolysis yield and reaction time. At 650 °C, AlF_3 was completely hydrolyzed in 1 h. Therefore, the optimal hydrolysis time was set to 1 h to ensure the complete hydrolysis of AlF_3. The solid products were characterized by means of XRD. As shown in Fig. 2, AlF_3 was entirely converted into α-Al_2O_3 at 650 °C in 1 h. As these results were satisfactory, it was unnecessary to use an accelerator.

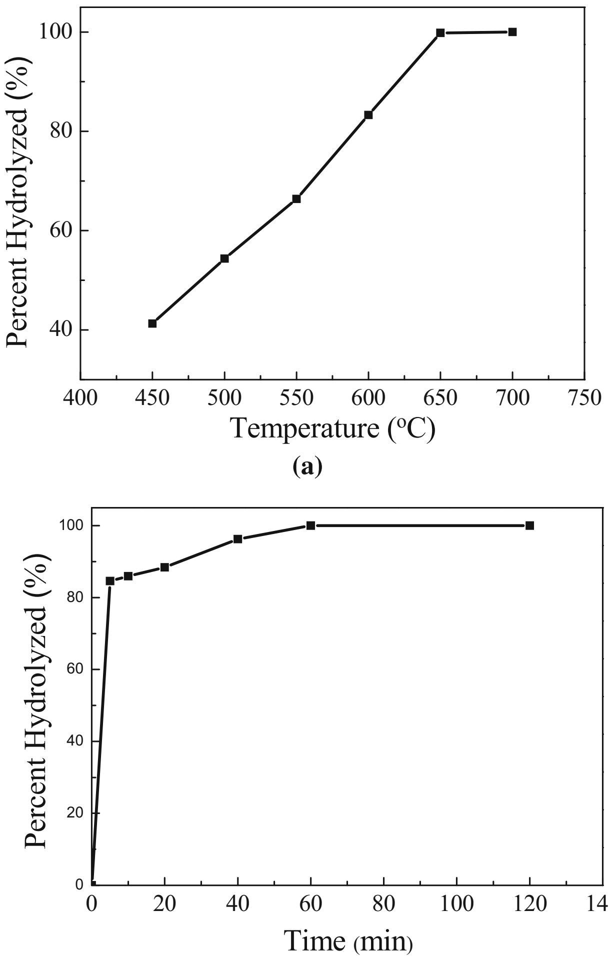

(a)

(b)

Fig. 1 Pyrohydrolysis of AlF_3 as a function of the reaction temperature and reaction time: **a** pyrohydrolysis of AlF_3 as a function of the reaction temperature, **b** pyrohydrolysis of AlF_3 as a function of the reaction time

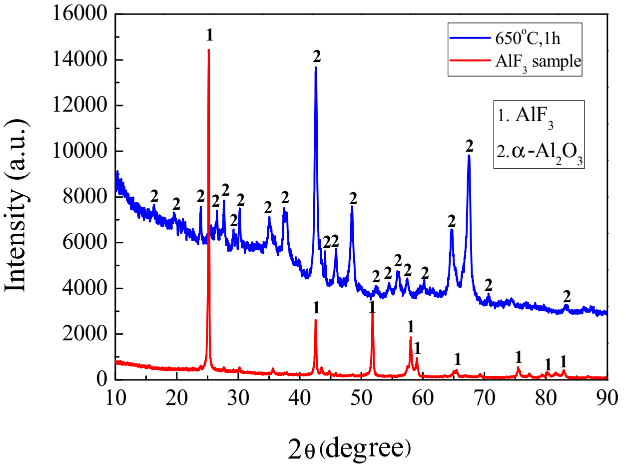

Fig. 2 (Color online) XRD patterns of the sample and the pyrohydrolysis product of AlF_3

The reaction mechanism was assumed to be as follows:

$$2AlF_3 + 3H_2O \rightarrow \alpha\text{-}Al_2O_3 + 6HF. \quad (1)$$

3.2 Pyrohydrolysis of LiF

Previous studies [5] revealed that AlF_3, a readily hydrolyzable fluoride, requires low hydrolysis temperature. In contrast, the fluoride LiF cannot be easily hydrolyzed and requires high reaction temperature. In the present study, the hydrolysis behavior of LiF at 650 °C was examined. The result showed that LiF was not hydrolyzable in 1 h, even when the pyrohydrolysis time was prolonged to 3 h. The XRD patterns of the samples before and after treatment are shown in Fig. 3. The high hydrolysis

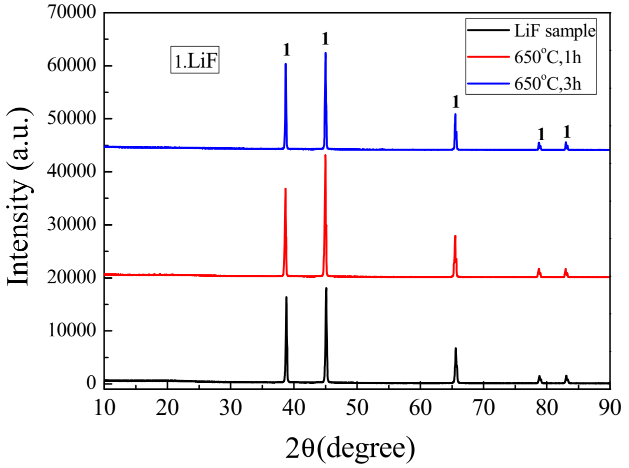

Fig. 3 (Color online) XRD patterns of the sample and the pyrohydrolysis product of LiF under different conditions

yield of fluorides within a short time confirmed that the reaction temperature and the absence of accelerators were the main factors limiting the pyrohydrolysis of LiF under the present experimental conditions. This necessitated the use of accelerators for the pyrohydrolysis of LiF.

3.3 Influence of the accelerator α-Al_2O_3 on the pyrohydrolysis of LiF

3.3.1 Effects of accelerator and reaction time on pyrohydrolysis

The effects of the amount of α-Al_2O_3 and the reaction time on the pyrohydrolysis of LiF were investigated. The solid products were characterized by XRD, as shown in Fig. 4a, b. The results showed that LiF was not completely hydrolyzed in 1 h, even when the mass ratio of accelerator to LiF was 6:1. In contrast, the use of a 5–1 weight ratio of accelerator to LiF with a reaction time of 3 h enabled LiF to be transformed completely. Hence, LiF could be converted by increasing the reaction time and the amount of accelerator. The XRD patterns showed that α-Al_2O_3 participated in the reaction of LiF in the form of $LiAlO_2$ and $LiAl_5O_8$ at different mass ratios. The final research results are summarized in Table 1.

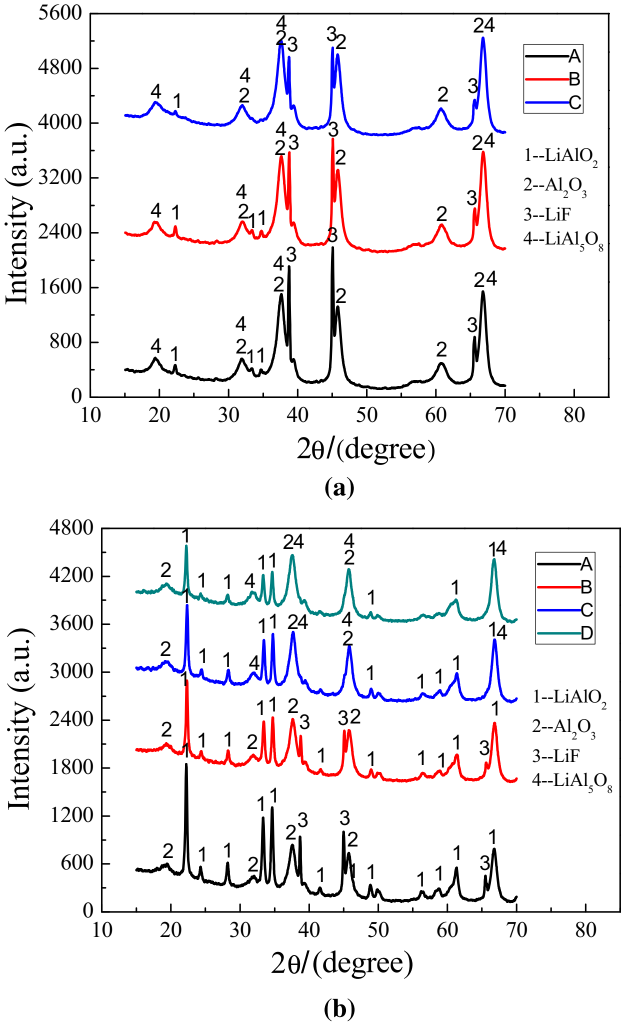

(a)

(b)

Fig. 4 (Color online) XRD patterns of the pyrohydrolysis products after **a** 1 h, **b** 3 h. In (**a**) mass ratio of α-Al_2O_3–LiF is (A) 4:1, (B) 5:1, and (C) 6:1. In (**b**) mass ratio of α-Al_2O_3–LiF is (A) 3:1, (B) 4:1, (C) 5:1, and (D) 6:1

3.3.2 Mechanism inference

When cryolite was pyrohydrolyzed in the presence of α-Al_2O_3, Silverman [24] presumed the reaction to resemble the following,

$$Na_3AlF_6 + 3H_2O + 11Al_2O_3 \rightarrow 6HF + Na_2O \cdot 11Al_2O_3 + NaAlO_2. \tag{2}$$

Thus, substances similar to $Na_2O \cdot nAl_2O_3$ and $NaAlO_2$ are produced when α-Al_2O_3 is used as an accelerator in the pyrohydrolysis of LiF. However, XRD showed that the main pyrohydrolysis product of LiF was $LiAlO_2$ when a small amount of α-Al_2O_3 was used, whereas large amounts of the accelerator produced $LiAlO_2$ and $LiAl_5O_8$ because the excess α-Al_2O_3 might react with $LiAlO_2$ to form $LiAl_5O_8$.

The following probable reaction processes may be considered:

When a small amount of α-Al_2O_3 was used:

$$2LiF + \alpha\text{-}Al_2O_3 + H_2O \rightarrow 2LiAlO_2 + 2HF. \tag{3}$$

When a large amount of α-Al_2O_3 was used:

$$2LiF + 5\alpha\text{-}Al_2O_3 + H_2O \rightarrow 2LiAl_5O_8 + 2HF, \tag{4}$$

which is

$$2LiF + \alpha\text{-}Al_2O_3 + H_2O \rightarrow 2LiAlO_2 + 2HF, \tag{5}$$

$$LiAlO_2 + 2\alpha\text{-}Al_2O_3 \rightarrow LiAl_5O_8, \tag{6}$$

$$(5) + (6) = (7)$$
$$2LiF + 5\alpha\text{-}Al_2O_3 + H_2O \rightarrow 2LiAl_5O_8 + 2HF. \tag{7}$$

Table 1 Influence of α-Al_2O_3 on pyrohydrolysis of LiF

Mass ratio (α-Al_2O_3–LiF)	3:1	4:1	5:1	6:1
1 h	+	+	+	+
3 h	+	+	++	++

(+ incompletely hydrolyzed, ++ completely hydrolyzed)

3.4 Influence of AlF_3 on pyrohydrolysis of LiF

3.4.1 Effect of AlF_3 and reaction time on pyrohydrolysis

The above-mentioned results showed that α-Al_2O_3, which could act as an accelerator, was the hydrolyzed product of AlF_3. Thus, we investigated the effects of AlF_3 on the dosage and reaction time of the pyrohydrolysis of LiF. The solid hydrolyzates were characterized by XRD analysis as shown in Fig. 5a, b. It can be seen that LiF was not completely hydrolyzed in 1 h even when the mass ratio of AlF_3–LiF was 10:1. However, increasing the mass ratio from 4:1–6:1 to 10:1 made it possible to completely hydrolyze LiF in 3 h. This result indicated that adding an appropriate amount of AlF_3 and prolonging the reaction time could facilitate the completion of the hydrolysis of LiF. Based on the XRD patterns, $LiAlO_2$ and $LiAl_5O_8$ would form in the reaction of LiF in the presence of different weight ratios of α-Al_2O_3. The final results are summarized in Table 2.

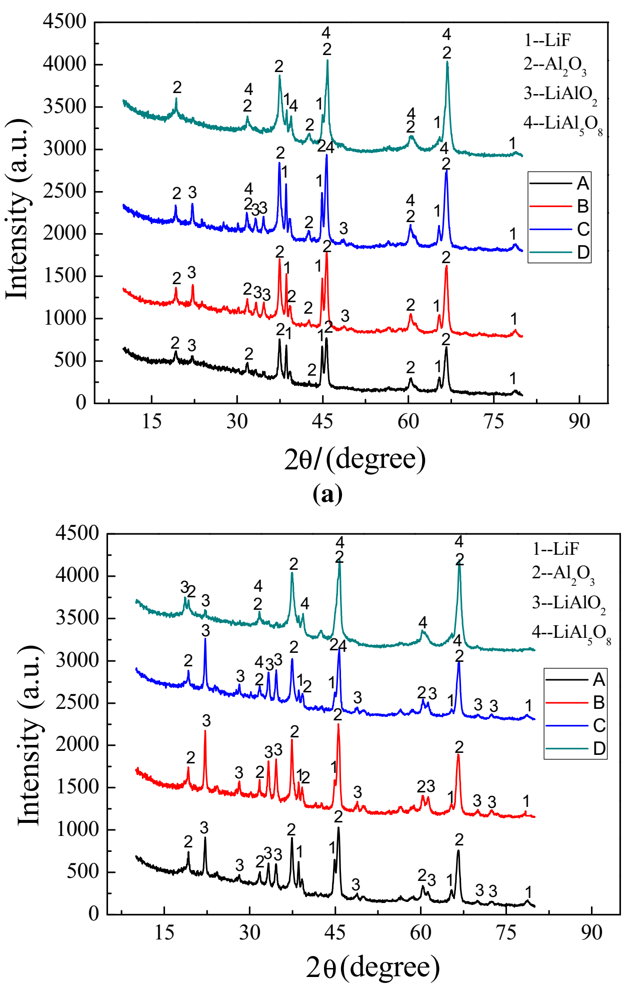

(a)

(b)

Fig. 5 (Color online) XRD patterns of the pyrohydrolysis products for **a** 1 h, **b** 3 h. In (**a**) mass ratio of AlF_3–LiF is (A) 4:1, (B) 5:1, (C) 6:1, (D) 10:1. In (**b**) mass ratio of AlF_3–LiF is (A) 4:1, (B) 5:1, (C) 6:1, (D) 10:1

3.4.2 Mechanism inference

Limited literature is available regarding the use of AlF_3 as an accelerator and its reaction mechanism in pyrohydrolysis. In particular, adding appropriate amounts of AlF_3 could contribute to the completion of the pyrohydrolysis. According to the aforementioned results obtained by using α-Al_2O_3 as an accelerator, we could speculate reasonably that AlF_3 could promote the pyrohydrolysis of LiF because α-Al_2O_3 is produced by the pyrohydrolysis. Furthermore, the final solid product, when adding AlF_3–LiF, was the same as adding α-Al_2O_3. Therefore, our speculation was verified. We could summarize the reaction mechanism as follows:

When a small amount of AlF_3 was used:

$$2AlF_3 + 3H_2O \rightarrow \alpha\text{-}Al_2O_3 + 6HF, \qquad (8)$$

$$2LiF + \alpha\text{-}Al_2O_3 + H_2O \rightarrow 2LiAlO_2 + 2HF, \qquad (9)$$

$$(8) + (9) = (10) \quad LiF + AlF_3 + 2H_2O \rightarrow LiAlO_2 + 4HF. \qquad (10)$$

When a large amount of AlF_3 was used:

$$2AlF_3 + 3H_2O \rightarrow \alpha\text{-}Al_2O_3 + 6HF, \qquad (11)$$

$$2LiF + \alpha\text{-}Al_2O_3 + H_2O \rightarrow 2LiAlO_2 + 2HF, \qquad (12)$$

$$LiAlO_2 + 2\alpha\text{-}Al_2O_3 \rightarrow LiAl_5O_8, \qquad (13)$$

$$(11) + (12) + (13) = (14) \quad LiF + 5AlF_3 + 8H_2O \rightarrow LiAl_5O_8 + 16HF. \qquad (14)$$

3.5 Pyrohydrolysis of Li_3AlF_6 molten salt

3.5.1 Pyrohydrolysis of Li_3AlF_6 molten salt in different components

LiF and AlF_3 may produce stable cryolite compounds [19–22]. In our previous work, molten salt with a certain proportion of Li_3AlF_6 was prepared using a mole ratio corresponding to the lowest melting point at which the eutectic salt was formed. Different proportions of the

Table 2 Influence of AlF_3 on pyrohydrolysis of LiF

Mass ratio (AlF_3–LiF)	4:1	5:1	6:1	10:1
1 h	+	+	+	+
3 h	+	+	+	++

(+ incompletely hydrolyzed, ++ completely hydrolyzed)

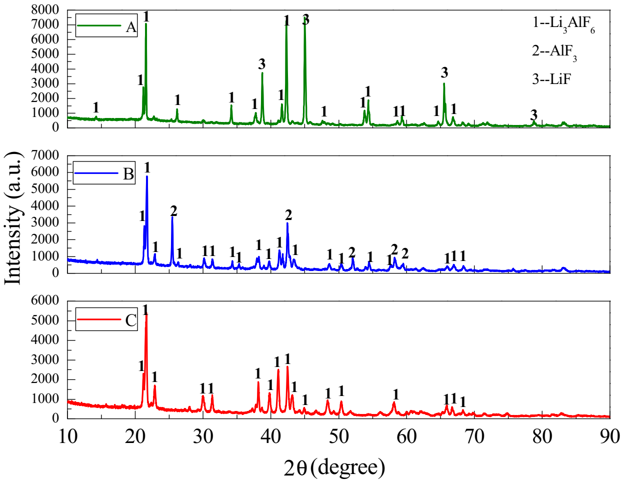

Fig. 6 (Color online) XRD patterns for different molar ratio of LiF–AlF_3 molten salt. **a**–Sample A (Li_3AlF_6 and excess LiF), **b** Sample B (Li_3AlF_6 and excess AlF_3), **c** Sample C (Li_3AlF_6, guaranteed to be 99% pure)

prepared molten salts and the procured cryolithionites were analyzed with XRD, and the results can be seen in Fig. 6. Based on the XRD patterns, the first batch of the molten salt in the experiment was composed of Li_3AlF_6 and excess LiF (Sample A), the second contained Li_3AlF_6 and excess AlF_3 (Sample B). The purity of the procured cryolithionite was 99%, and its main constituent was Li_3AlF_6 (Sample C).

The three molten salt samples were hydrolyzed at 650 °C for 1 h and the hydrolysates characterized by XRD analysis. These results are detailed in Table 3 and Fig. 7a–c. The final hydrolysates of Samples A and C were Al_2O_3 and LiF (Fig. 7a, c), indicating the incomplete hydrolysis of these samples. The results were consistent even when the reaction time was prolonged to 3 h. Meanwhile, Sample B was completely hydrolyzed in 1 h, and the final hydrolysate was $LiAlO_2$ (Fig. 7b). Further analysis showed that the final hydrolysate of Samples A and C was γ-Al_2O_3, whereas that of the sample containing excess AlF_3 was α-Al_2O_3. This indicates that Sample B may be completely hydrolyzed with the acceleration effect of α-Al_2O_3.

3.5.2 *Mechanism inference*

Silverman reported that the solid hydrolysates of Na_3AlF_6 were $NaAlO_2$ and NaF [24]. The general pyrohydrolysis reaction of Na_3AlF_6 could be expressed as follows:

$$Na_3AlF_6 + 2H_2O = NaAlO_2 + 2NaF + 4HF. \tag{15}$$

In comparison, in our experiment, the XRD results showed that the main hydrolysates of Samples A (Li_3AlF_6 and excess LiF) and C (Li_3AlF_6, guaranteed to be 99% pure) were Al_2O_3 and LiF. Sample B (Li_3AlF_6 and excess AlF_3) yielded $LiAlO_2$ only because of an excess of AlF_3. Thus, the reaction of Li_3AlF_6 is assumed to be as follows, when the Li_3AlF_6 is pure or with an excess of LiF (Samples A and C),

$$2Li_3AlF_6 + 3H_2O \rightarrow Al_2O_3 + 6LiF + 6HF. \tag{16}$$

when Li_3AlF_6 is used with an excess of AlF_3 (Sample B),

$$Li_3AlF_6 + 2H_2O \rightarrow LiAlO_2 + 2LiF + 4HF, \tag{17}$$

$$2AlF_3 + 3H_2O \rightarrow \alpha\text{-}Al_2O_3 + 6HF, \tag{18}$$

$$2LiF + \alpha\text{-}Al_2O_3 + H_2O \rightarrow 2LiAlO_2 + 2HF, \tag{19}$$

$$\begin{aligned}(17)+(18)+(19)=(20):\ \ & Li_3AlF_6 + 2AlF_3 + 6H_2O \\ & \rightarrow 3LiAlO_2 + 12HF.\end{aligned} \tag{20}$$

3.6 Influence of AlF_3 and accelerator α-Al_2O_3 on pyrohydrolysis of Li_3AlF_6

Complete hydrolysis was difficult to achieve because the direct hydrolysate of pure Li_3AlF_6 might produce LiF. Therefore, the effects of AlF_3 and the accelerator α-Al_2O_3 on the pyrohydrolysis of Li_3AlF_6 were explored. Figure 8 shows the XRD patterns of the solid hydrolysates. The results showed that adding appropriate amounts of α-Al_2O_3

Table 3 Different molar ratio of LiF–AlF_3 molten salt

	Sample A (LiF–AlF_3)	Sample B (LiF–AlF_3)	Sample C (purchased)
Molar ratio	85:15	66:34	75:25
Mass ratio	7:4	3:5	13:14
Reaction time (h)	12	12	–
Maximum reaction temperature (°C)	900	900	–
Molten salt components (characterized by XRD)	Li_3AlF_6, LiF	Li_3AlF_6, AlF_3	Li_3AlF_6 (pure 99%)
Pyrohydrolysis condition	650 °C, 1 h	650 °C, 1 h	650 °C, 1 h
Solid products after pyrohydrolysis	Al_2O_3, LiF	$LiAlO_2$	Al_2O_3, LiF

Fig. 7 (Color online) XRD patterns of the pyrohydrolysis products of Li_3AlF_6 samples. **a** Sample A (Li_3AlF_6 and excess LiF), **b** Sample B (Li_3AlF_6 and excess AlF_3), **c** Sample C (Li_3AlF_6, guaranteed to be 99% pure)

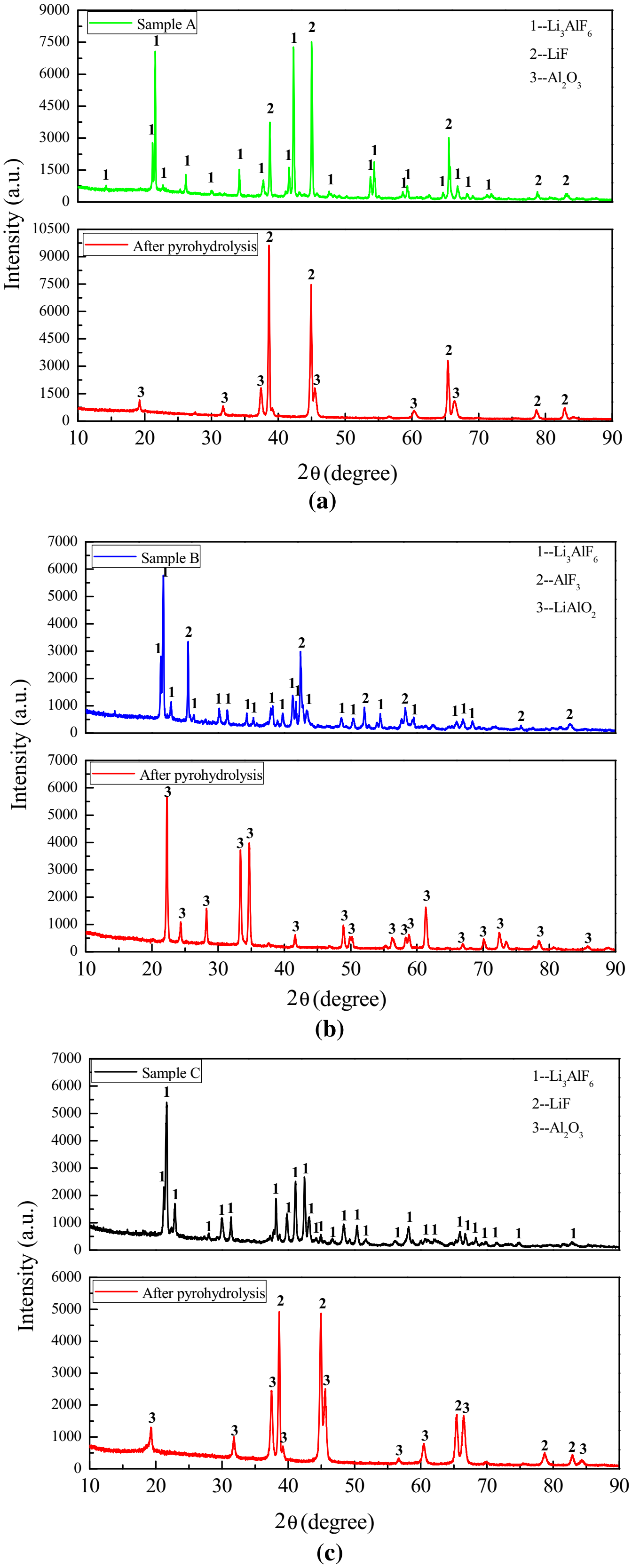

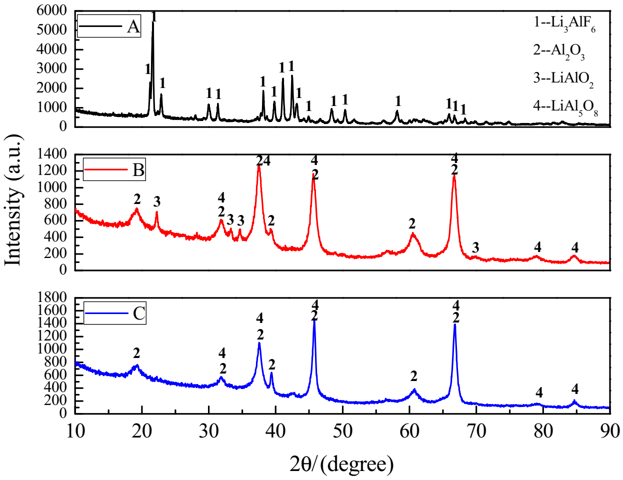

Fig. 8 (Color online) XRD patterns of pyrohydrolysis products of Li_3AlF_6 sample with α-Al_2O_3 and AlF_3. **a** Li_3AlF_6 sample, **b** Li_3AlF_6 sample mix with α-Al_2O_3, **c** Li_3AlF_6 sample mix with AlF_3

(the mass ratio of the accelerator to the sample was 3:1) and AlF_3 (the mass ratio of AlF_3 to the sample was 6:1) might trigger the reaction of Li_3AlF_6 until the hydrolysis was completed. Based on the XRD patterns, adding α-Al_2O_3 produced $LiAlO_2$ and $LiAl_5O_8$, whereas adding AlF_3 yielded $LiAl_5O_8$ and Al_2O_3.

3.6.1 Mechanism inference

Based on the results of the effects of AlF_3 and α-Al_2O_3 on the pyrohydrolysis of LiF and the reaction mechanism on cryolite proposed by Silverman [24], the reaction mechanisms of α-Al_2O_3 and AlF_3 for the pyrohydrolysis of Li_3AlF_6 were deduced as follows.

The mechanism of the reaction of Li_3AlF_6 with α-Al_2O_3:

$$\mathrm{Li_3AlF_6 + 2H_2O \rightarrow LiAlO_2 + 2LiF + 4HF}, \tag{21}$$

$$\mathrm{2LiF + \alpha\text{-}Al_2O_3 + H_2O \rightarrow 2LiAlO_2 + 2HF}, \tag{22}$$

$$\mathrm{LiAlO_2 + 2\alpha\text{-}Al_2O_3 \rightarrow LiAl_5O_8}, \tag{23}$$

$$(21) + (22) + (23) = (24)$$

$$\mathrm{Li_3AlF_6 + 3\alpha\text{-}Al_2O_3 + 3H_2O \rightarrow 2LiAlO_2 + LiAl_5O_8 + 6HF}. \tag{24}$$

The mechanism of the reaction of Li_3AlF_6 with AlF_3:

$$\mathrm{Li_3AlF_6 + 2H_2O \rightarrow LiAlO_2 + 2LiF + 4HF}, \tag{25}$$

$$\mathrm{2AlF_3 + 3H_2O \rightarrow \alpha\text{-}Al_2O_3 + 6HF}, \tag{26}$$

$$\mathrm{2LiF + \alpha\text{-}Al_2O_3 + H_2O \rightarrow 2LiAlO_2 + 2HF}, \tag{27}$$

$$\mathrm{LiAlO_2 + 2\alpha\text{-}Al_2O_3 \rightarrow LiAl_5O_8}, \tag{28}$$

$$(25) + (26) + (27) + (28) = (29)$$

$$\mathrm{Li_3AlF_6 + 14AlF_3 + 24H_2O \rightarrow 3LiAl_5O_8 + 48HF}. \tag{29}$$

4 Conclusion

The pyrohydrolysis behavior and reaction mechanism of LiF, AlF_3, and Li_3AlF_6 were investigated. The effects of AlF_3 and α-Al_2O_3 on the pyrohydrolysis of LiF and Li_3AlF_6 were explored. These results are expected to serve as an important guideline for future experiments on the molten salt LiF–BeF_2 and the pyrohydrolysis of multi-component molten salt mixtures. The following conclusions were drawn:

1. The pyrohydrolysis efficiency of AlF_3 increased with increasing reaction temperature and time. After pyrohydrolysis at 650 °C for 1 h, AlF_3 was completely hydrolyzed and converted to α-Al_2O_3.
2. LiF cannot be hydrolyzed in 1 or 3 h, at 650 °C. The addition of AlF_3 and the accelerator α-Al_2O_3 promoted the completely pyrohydrolysis of LiF.
3. The results showed that neither Sample A (Li_3AlF_6 and excess LiF) nor C (Li_3AlF_6, guaranteed to be 99% pure) may be completely hydrolyzed, and their final hydrolysates were γ-Al_2O_3 and LiF, respectively. Sample B (Li_3AlF_6 and excess AlF_3) could be completely hydrolyzed and converted into $LiAlO_2$.
4. Adding appropriate amounts of AlF_3 and α-Al_2O_3 could accelerate the complete hydrolysis of Li_3AlF_6.

In consideration of the diagonal effect, according to which the chemical properties of BeF_2 and AlF_3 are similar, we presumed that the behavior of AlF_3 could be extended to BeF_2. We verified the feasibility of converting AlF_3–Al_2O_3, which can be used as an accelerator in the pyrohydrolysis reaction. Our results suggest that BeF_2 can act as an accelerator with a self-accelerating effect when reprocessing spent TMSR fuel.

References

1. J.X. Zuo, C.M. Zhang, The introduction of the safety of molten salt reactor. Nucl. Saf. **3**, 73–78 (2011). https://doi.org/10.3969/j.issn.1672-5360.2011.03.013
2. K.P. Wang, J.X. Zuo, J.P. Jing et al., Safety margin analysis of thorium molten salt reactor with solid fuel. Sci. Technol. Eng. **3**, 179–182 (2016). https://doi.org/10.3969/j.issn.1671-1815.2016.03.033
3. M.H. Jiang, H.J. Xu, Z.M. Dai, Advanced fission energy program-TMSR nuclear energy system. Bull. CAS **27**, 366–374 (2012). https://doi.org/10.3969/j.issn.1000-3045.2012.03.016

4. R.M. Sawant, M.A. Mahajan, P. Verma et al., Fluoride determination in various matrices relevant to nuclear industry: a review. Radiochim. Acta **95**, 585–594 (2007). https://doi.org/10.1524/ract.2007.95.10.585
5. J.C. Waft, W.D. Cline, R.D. Tevebaugh, Pyrohydrolysis in the determination of fluoride and other halides. Anal. Chem. **26**, 342–346 (1954). https://doi.org/10.1021/ac60086a019
6. B.X. Peng, D.S. Wu, Simultaneous rapid determination of halogens in clay using pyrohydrolysis combined with ion chromatography. Chin. J. Anal. Chem. **41**, 1499–1504 (2013). https://doi.org/10.1016/j.fuel.2011.12.011
7. A. Pandey, A. Kelkar, R.K. Singhal et al., Effect of accelerators on thoria based nuclear fuels for rapid and quantitative pyrohydrolytic extraction of F^- and Cl^- and their simultaneous determination by ion chromatography. J. Radioannal. Nucl. Chem. **29**, 3743–3749 (2012). https://doi.org/10.1007/s10967-012-1672-7
8. T. Taflik, F.A. Duarte, É.L.M. Flores et al., Determination of bromine, fluorine and iodine in mineral supplements using pyrohydrolysis for sample preparation. J. Braz. Chem. Soc. **23**, 488–495 (2012). https://doi.org/10.1590/S0103-50532012000300016
9. R.H. Powell, O. Menis, Separation of fluoride from inorganic compounds by pyrolysis. Anal. Chem. **30**, 1546–1549 (1958). https://doi.org/10.1021/ac60141a032
10. C.D. Susano, J.C. White, J.E. Lee, Apparatus for the pyrohydrolytic determination of fluoride and other halides. Anal. Chem. **27**, 453–454 (1955). https://doi.org/10.1021/ac60099a042
11. I. Matae, I. Niro, Pyrohydrolysis reactions of UF_4 and UO_2F_2 effect of oxygen on reactions. J. Nucl. Sci. Technol. **20**, 400–404 (1983). https://doi.org/10.1080/18811248.1983.9733409
12. N.R. Hofmann, J.N.G. Paniz, E.M. de Moraes et al., Determination of halogens in cardboard gaskets using pyrohydrolysis. Anal. Lett. **49**, 1903–1916 (2016). https://doi.org/10.1080/00032719.2015.1126599
13. X.Y. Dong, X.B. Zheng, Y.L. Song et al., Pyrohydrolysis of uranium tetrafluoride and thorium tetrafluoride. J. Nucl. Radiochem. **36**, 181–185 (2014). https://doi.org/10.7538/hhx.2014.36.03.0181
14. J. Peng, X.B. Zheng, T.T. Qiu et al., Pyrohydrolysis of SmF_3 in moist air. J. Fluor. Chem. **193**, 106–112 (2017). https://doi.org/10.1016/j.jfluchem.2016.11.011
15. M. Ponikvar, J.F. Liebman, Paradoxes and paradigms: observations on pyrohydrolytic decomposition of fluorine-containg materials and accompanying thermochemistry. Struct. Chem. **17**, 75–78 (2006). https://doi.org/10.1007/s11224-006-9023-3
16. R.M. Sawant, M.A. Mahajan, D.J. Shah et al., Pyrohydrolytic separation technique for fluoride and chloride from radioactive liquid wastes. J. Radioannal. Nucl. Chem. **287**, 423–426 (2011). https://doi.org/10.1007/s10967-010-0698-y
17. V.B. Charles, E.B. Keith, W.O. Laughlin, The determination of fluorine in rare earth fluorides by high temperature hydrolysis. Anal. Chim. Acta **19**, 239–243 (1958). https://doi.org/10.1016/S0003-2670(00)88149-0
18. B. Nebesar, The high-temperature analytical uses of vanadium(V) oxide. Tala **25**, 185–194 (1978). https://doi.org/10.1016/0039-9140(78)80003-4
19. K. Matiasovský, M. Paucirova, M. Malinovský, Volume properties of molten ternary LiF–Li_3 AlF_6–Na_3AlF_6 mixtures. Collect. Czech. Chem. Commun. **35**, 907–914 (1970). https://doi.org/10.1135/cccc19700907
20. O. Conocar, N. Douyere, J. Lacquement, Extraction behavior of actinides and lanthanides in a molten fluoride/liquid aluminum system. J. Nucl. Mater. **344**, 136–141 (2005). https://doi.org/10.1016/j.jnucmat.2005.04.031
21. E.W. Dewing, Thermodynamic functions for LiF–AlF_3 mixtures at 1293 K. Metall. Mater. Trans. B **11**, 245–249 (1980). https://doi.org/10.1007/BF02668408
22. E.W. Dewing, Thermodynamics of the system LiF–AlF_3. J. Electrochem. Soc. **123**, 1289–1294 (1976). https://doi.org/10.1149/1.2133062
23. G.Q. Zong, Z.H. Cui, X.G. Sun et al., One-step synthesis of high-purity Li_2BeF_4 molten salt. J. Fluor. Chem. **181**, 30–35 (2016). https://doi.org/10.1002/chin.201613013
24. H.P. Silverman, F.J. Bowen, Pyrohydrolysis of cryolite fluoride-bearing materials. Anal. Chem. **31**, 160–165 (1960). https://doi.org/10.1021/ac60156a021